

Increased Remyelination and Proregenerative Microglia Under Siponimod Therapy in Mechanistic Models

Michael Dietrich, PhD,* Christina Hecker, MSc,* Elodie Martin, PhD, Dominique Langui, PhD, Michael Gliem, MD, Bruno Stankoff, MD, PhD, PU-PH, Catherine Lubetzki, MD, PhD, PU-PH, Joel Gruchot, MSc, Peter Göttle, PhD, Andrea Issberner, Milad Nasiri, MD, Pamela Ramseier, Christian Beerli, Sarah Tisserand, MSc, Nicolau Beckmann, PhD, Derya Shimshek, PhD, Patrick Petzsch, PhD, David Akbar, MSc, Bodo Levkau, Prof., Holger Stark, Prof., Karl Köhrer, Prof., Hans-Peter Hartung, Prof., Patrick Küry, Prof., Sven Günther Meuth, Prof., Marc Bigaud, PhD, Bernard Zalc, Prof.,† and Philipp Albrecht, Prof.†

Correspondence
Dr. Albrecht
phil.albrecht@gmail.com

Neurol Neuroimmunol Neuroinflamm 2022;9:e1161. doi:10.1212/NXI.000000000001161

Abstract

Background and Objectives

Siponimod is an oral, selective sphingosine-1-phosphate receptor-1/5 modulator approved for treatment of multiple sclerosis.

Methods

Mouse MRI was used to investigate remyelination in the cuprizone model. We then used a conditional demyelination *Xenopus laevis* model to assess the dose-response of siponimod on remyelination. In experimental autoimmune encephalomyelitis–optic neuritis (EAEON) in C57Bl/6J mice, we monitored the retinal thickness and the visual acuity using optical coherence tomography and optomotor response. Optic nerve inflammatory infiltrates, demyelination, and microglial and oligodendroglial differentiation were assessed by immunohistochemistry, quantitative real-time PCR, and bulk RNA sequencing.

Results

An increased remyelination was observed in the cuprizone model. Siponimod treatment of demyelinated tadpoles improved remyelination in comparison to control in a bell-shaped dose-response curve. Siponimod in the EAEON model attenuated the clinical score, reduced the retinal degeneration, and improved the visual function after prophylactic and therapeutic treatment, also in a bell-shaped manner. Inflammatory infiltrates and demyelination of the optic nerve were reduced, the latter even after therapeutic treatment, which also shifted microglial differentiation to a promyelinating phenotype.

Discussion

These results confirm the immunomodulatory effects of siponimod and suggest additional regenerative and promyelinating effects, which follow the dynamics of a bell-shaped curve with high being less efficient than low concentrations.

*Equally contributing first authors.

†Equally contributing senior authors.

From the Department of Neurology (M.D., C.H., M.G., J.G., P.G., A.I., M.N., H.-P.H., P.K., S.G.M.), Heinrich Heine University Düsseldorf, Medical Faculty (P.A.), Düsseldorf, Germany; Sorbonne Université (E.M., D.L., B.S., C.L., D.A., B.Z.), Inserm, CNRS, Institut du Cerveau, Pitié-Salpêtrière Hospital; AP-HP (B.S.), Saint-Antoine Hospital; AP-HP (C.L.), Pitié-Salpêtrière Hospital, Paris, France; Novartis Institutes for BioMedical Research (P.R., C.B., S.T., N.B., D.S., M.B.), Basel, Switzerland; Biological and Medical Research Center (BMFZ) (P.P., K.K.), Heinrich Heine University Düsseldorf, Medical Faculty; Institute for Molecular Medicine III (B.L.), University Hospital Düsseldorf and Heinrich Heine University Düsseldorf; Institute of Pharmaceutical and Medicinal Chemistry (H.S.), Heinrich Heine University Düsseldorf, Düsseldorf, Germany; Brain and Mind Center (H.-P.H.), University of Sydney, NSW, Australia; and Medical University of Vienna (H.-P.H.), Vienna, Austria.

Go to [Neurology.org/NN](https://www.neurology.org/NN) for full disclosures. Funding information is provided at the end of the article.

The Article Processing Charge was funded by the authors.

This is an open access article distributed under the terms of the Creative Commons Attribution-NonCommercial-NoDerivatives License 4.0 (CC BY-NC-ND), which permits downloading and sharing the work provided it is properly cited. The work cannot be changed in any way or used commercially without permission from the journal.

Glossary

ANOVA = analysis of variance; **Arg-1** = arginase-1; **AUC** = area under the curve; **BAF312/Sip** = siponimod; **BW** = bodyweight; **c/d** = cycles per degree; **CC** = corpus callosum; **DEG** = differentially expressed gene; **dpi** = days postimmunization; **EAE(ON)** = experimental autoimmune encephalomyelitis (optic neuritis); **EAEON** = experimental autoimmune encephalomyelitis–optic neuritis; **FDR** = false discovery rate; **GCL** = ganglion cell layer; **GFAP** = glial fibrillary acidic protein; **IPL** = inner plexiform layer; **IRL** = inner retinal layer; **LC/MS/MS** = liquid chromatography/tandem mass spectrometry; **MBP** = myelin basic protein; **MOG35-55** = myelin oligodendrocyte glycoprotein fragment 35-55; **MS** = multiple sclerosis; **MTR** = magnetization transfer ratio; **MTZ** = metronidazole; **NTR** = nitroreductase; **OCT** = optical coherence tomography; **OMR** = optomotor response; **OPC** = oligodendrocyte precursor cell; **PDGFR α** = platelet-derived growth factor receptor A; **RGC** = retinal ganglion cell; **RNFL** = retinal nerve fiber layer; **S1P1/5** = sphingosine-1-phosphate receptor 1 and 5; **SPMS** = secondary progressive multiple sclerosis; **T2-WSI** = T2-weighted signal intensity; **TNF- α** = tumor necrosis factor alpha; **Ym1/Chi3l3** = chitinase 3-like-3.

Siponimod, a potent and highly selective sphingosine-1-phosphate receptor 1 and 5 (S1P1/5) modulator, is a disease-modifying therapy that significantly reduced disability progression, cognitive decline, and total brain volume loss vs placebo in patients with secondary progressive multiple sclerosis (SPMS), as demonstrated in the phase III EXPAND study.¹ It has beneficial effects in the CNS of experimental autoimmune encephalomyelitis (EAE) mice that are independent of peripheral immune effects, suggesting that in addition to its anti-inflammatory effects, siponimod may be effective in limiting neurodegenerative pathologic processes in SPMS.²

Promoting remyelination is another key therapeutic strategy to limit disability progression and represents one of the major therapeutic challenges in MS. Therefore, experimental models to investigate substances promoting remyelination in vivo are of paramount interest.^{3,4} The cuprizone intoxication mouse model is a well-established mechanistic model to study remyelination processes.⁵ As oligodendrocyte precursor cells (OPCs) are not affected by cuprizone, they readily proliferate, migrate, differentiate, and integrate again into the circuitry resulting in remyelination after withdrawal. Novel data from a *Xenopus laevis* demyelination model indicated a remyelinating potential of siponimod. Optic neuritis (ON) presenting with reduction of visual function is frequent in MS and accompanied by retinal nerve fiber layer thinning and retinal ganglion cell (RGC) loss, which can be used as an outcome parameter for neuroprotection studies investigating ON as a model for acute inflammatory relapses.⁶⁻⁹ Therefore, in this innovative approach investigating the visual pathway of siponimod-treated EAE-associated ON (EAEON) mice, we used longitudinal visual system readouts, namely optical coherence tomography (OCT) and optomotor response (OMR), which are ideally suited to evaluate CNS degeneration in preclinical studies and clinical approaches.¹⁰⁻¹³

In this study, we assessed the impact of siponimod in 3 different animal models of demyelination: (1) a toxic cuprizone-induced demyelination mouse model, (2) a conditional demyelination of the optic nerve in transgenic *Xenopus laevis*, and (3) a myelin oligodendrocyte glycoprotein fragment

35-55 (MOG₃₅₋₅₅)-induced EAEON by visual system readouts, revealing yet unknown mechanisms on the shift of the microglial cell population toward a regenerative phenotype.

Methods

Cuprizone Intoxication Model and Measurement of C57Bl/6J Mice

Cuprizone preparation and randomization is described in the eMethods. In brief, female C57Bl/6J mice (8–10 weeks old from Charles River, Germany) received normal diet over 7 weeks (control group) or were fed with cuprizone-loaded pellets (2 g/kg food) for 5 weeks and then switched either to siponimod-loaded pellets (10 mg/kg food) over 2 weeks (cuprizone/siponimod group) or to drug-free pellets (cuprizone/sham group). MRI measurements were performed at weeks 5, 6, and 7 and histology on week 7 with LFB and GST- π as described in the eMethods, [links.lww.com/NXI/A706](https://www.lww.com/NXI/A706).

Xenopus laevis Demyelination Model

To test the effect of siponimod on remyelination in vivo, we used a conditional demyelination transgenic model, Tg(mbp:GFP-NTR), developed in *Xenopus laevis* as described before¹⁴⁻¹⁶ and in the eMethods. Before the quantification of GFP+ cells, we anesthetized the tadpoles of either sex in 0.05% MS-222 (ethyl-3-aminobenzoate methanesulfonate; Sigma-Aldrich) and returned them to standard water conditions for recovery. Tadpoles were euthanized in 0.5% MS-222 before the optic nerve was dissected.

For regeneration experiments, metronidazole (MTZ)-exposed animals (MTZ preparation described in the eMethods) were allowed to recover for 3 days in either normal water (control) or water containing siponimod at increasing concentrations in ambient laboratory lighting (12 hours light/12 hours dark).

Induction of EAEON and Treatment of C57Bl/6J Mice

EAEON was induced in female, 6-week-old C57Bl/6J by 200 μ g MOG₃₅₋₅₅ (Biotrend, Germany) immunization followed by intraperitoneal injections of 200 ng of pertussis toxin

(Sigma-Aldrich, Germany) at days 0 and 2 as previously described.¹⁷ Mice were fed with siponimod-loaded pellets at 0.01 or 0.03 g/kg of food, leading to a daily drug intake of approximately 2 and 6 mg/kg bodyweight, respectively (considering a mean daily food intake of 3 g/mouse).¹⁸⁻²¹ Treatment was started at the same day (d0), 14 days (d14), or 30 days (d30) after MOG₃₅₋₅₅ immunization. The clinical EAE score was graded daily as described previously.¹⁷

OCT and OMR in Mice

The measurements of retinal layers were performed using a Spectralis HRA + OCT device (Heidelberg Engineering, Germany) with several adaptations for rodents.²² The analysis and scanning protocols are described elsewhere^{11,23} and in the eMethods, links.lww.com/NXI/A706, in line with the APOSTEL recommendations.²⁴ Visual function analysis was performed with a testing chamber and OptoMotry software from CerebralMechanics, Canada, as previously described^{23,25} and explained in detail in the eMethods, links.lww.com/NXI/A706.

Histologic Analysis

Wholemount of the *Xenopus* Optic Nerve and Analysis

Tadpoles were fixed by immersion in 4% paraformaldehyde for 1 hour at room temperature. Fixed optic nerves were carefully dissected out and processed as described in the eMethods. In brief, oligodendrocytes were stained with anti-GFP (1:1,000, Aves Lab) and microglial cells with *Bandeiraea simplicifolia isolectin B4* (Alexa Fluor594-conjugated IB4, 1:1,000, Invitrogen), and images were acquired using the Olympus FV-1200 upright confocal microscope (Obj 20X-zoom 1.6).

Electron Microscopy of *Xenopus* Tadpole Optic Nerve

Xenopus larvae were fixed in a mixture of 2% paraformaldehyde, 2% glutaraldehyde, in 0.1 M cacodylate buffer pH 7.4 and 0.002% calcium chloride overnight at 4°C and processed as described in the eMethods, links.lww.com/NXI/A706. Ultrathin sections were examined on an HT7700 electron microscope (Hitachi) operated at 70 kV. Electron micrographs were taken using the integrated AMT XR41-B camera (2048X2048 pixels).

Quantification of GFP⁺ Cells in the *Xenopus* Optic Nerve

As described previously,¹⁶ GFP fluorescence was analyzed directly in vivo in *Xenopus* embryos using an AZ100 Nikon Multizoom Macro-Microscope. From the emergence of the optic nerve, directly after the chiasm, to the retinal end, the total number of GFP⁺ cells was counted independently by 2 researchers in a double-blinded manner. The counts were compared with control untreated animals of the same developmental stage.

Wholemounts and Histologic Optic Nerve Analysis of C57Bl/6J EAEON Mice

After 21, 35, or 90 days of EAEON, mice were killed, and eyes and optic nerves were extracted and processed as described in the eMethods.

Bulk RNA Sequencing of the Optic Nerve From EAEON Mice

RNA extraction was performed as previously described.²⁶ RNA was stored at -80°C until analysis as described in the eMethods, links.lww.com/NXI/A706.

qPCR Analysis of the Optic Nerve of EAEON C57Bl/6J Mice

RNA extraction, reverse transcription, and quantitative real-time PCR were performed as previously described²⁶ using Fam/Dark quencher probes from the Universal Probe Library (Roche, Switzerland) or individually designed Fam/Tamra probes (Eurofins Genomics, Germany). HPRT and GAPDH served as endogenous control genes. Primer sequences can be found in eTable 1, links.lww.com/NXI/A706.

Statistics

Statistical analysis was performed using Prism 5 (version 5.00, Graphpad Software, Inc.) and IBM SPSS Statistics (version 20, IBM Corporation, USA). A 2-tailed analysis of variance (ANOVA) with the Dunnett post hoc test was used to compare the area under the curve for the EAE scores and blood siponimod concentration time courses. qPCRs were analyzed using 2-way ANOVA with the Bonferroni post hoc test. Group means were compared by 1-way ANOVA with the Dunnett post hoc test using 1 eye per animal for the histologic investigations. Differences in retinal thickness and visual function were analyzed using generalized estimating equations with an exchangeable correlation matrix to adjust for intrasubject intereye correlations.

MRI data were analyzed using ANOVA with random effects (Systat version 13; Systat Software Inc., San Jose, CA) to take into account the longitudinal structure of the data. A value of $p < 0.05$ was considered significant. For the RNAseq, the statistical analysis is described in the eMethods, links.lww.com/NXI/A706.

Study Approval

C57Bl/6J Mice

The procedures were performed in accordance with the Animal Research: Reporting of In Vivo Experiments guidelines, approved by the regional authorities (State Agency for Nature, Environment and Consumer Protection; AZ 84-02.04.2016.A137) and conform to the Association for Research in Vision and Ophthalmology (ARVO) Statement for the Use of Animals in Ophthalmic and Vision Research. Cuprizone studies were approved by the Swiss Cantonal Veterinary Authority of Basel City, Switzerland (license BS-2711).

Xenopus laevis Tadpoles

Animal care was in compliance with institutional and national guidelines. All animal experiments conformed to the European Community Council directive (86/609/EEC) as modified (2010/603/UE) and have been approved by the ethical committee of the French Ministry of Higher Education and Research (APAFIS#5842-2016101312021965).

Data Availability

Data not provided in the article because of space limitations may be shared at the request of any qualified investigator for purposes of replicating procedures and results.

Results

Siponimod Promotes Remyelination After Cuprizone Intoxication

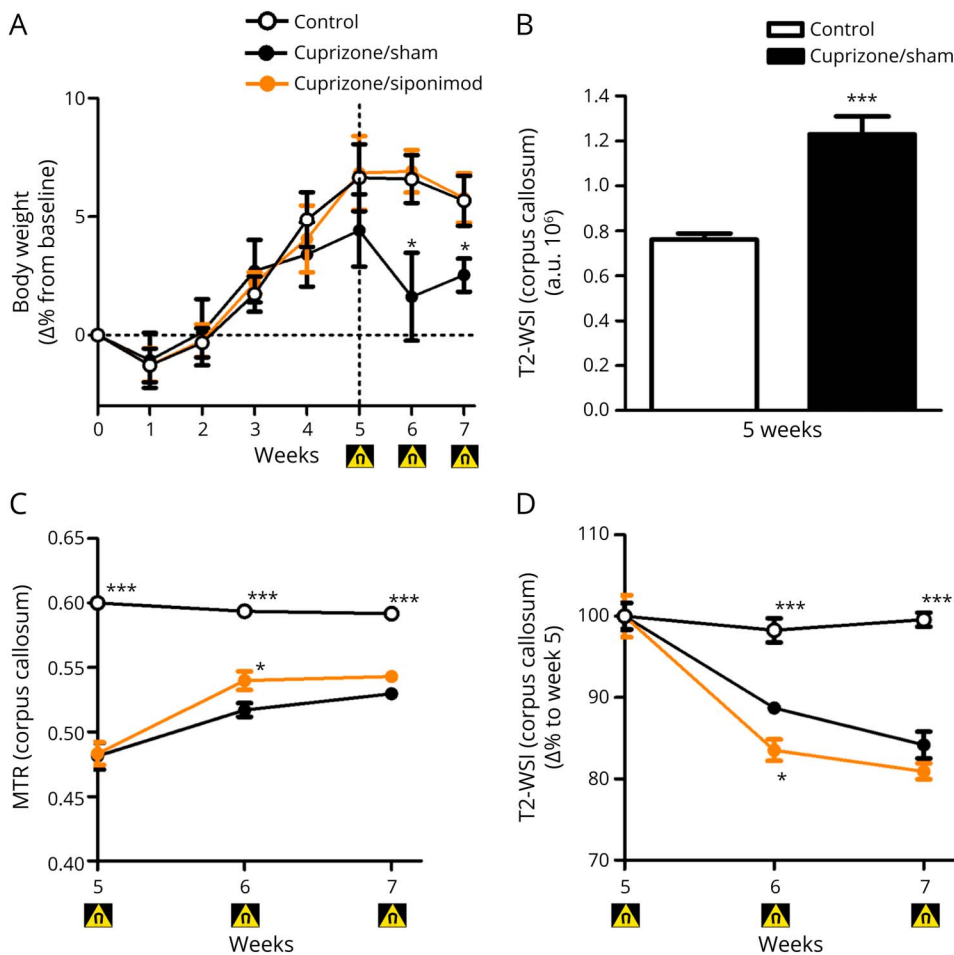
We used the cuprizone model of toxic demyelination to study siponimod's effects on remyelination in vivo. During the 5-week intoxication phase, no particular health issue could be detected in cuprizone-treated vs control mice, and similar longitudinal bodyweight changes vs baseline were observed in the 3 study groups (Figure 1A). Hence, at the start of the treatment, all 3 groups presented similar mean bodyweights (21.9 ± 0.4 g; 21.4 ± 0.4 g; and 22.2 ± 0.3 g).

Over the following 2 weeks, the mice that received drug-free pellets (cuprizone/sham group) showed a slight but significant loss in bodyweight vs controls. This was not observed in

mice that received siponimod-loaded pellets (cuprizone/siponimod group) (Figure 1A). In this group, the mean siponimod concentrations measured in blood and brain homogenates were within the expected ranges, that is, 0.41 ± 0.01 μ M and 2.7 ± 0.7 nmol/g (equivalent to 2.7 ± 0.7 μ M), respectively, confirming the success of the treatment.

As expected, cuprizone-intoxicated mice showed marked demyelination within their CC at week 5, as suggested by significantly decreased magnetization transfer ratio (MTR) in these regions when compared with values in control mice (Figure 1C). On cuprizone washout in weeks 5–7, MTR in mice fed with drug-free pellets increased in the CC (Figure 1C), suggesting spontaneous partial remyelination. This effect was particularly evident when calculating the area under the curve (AUC) (eFigure 1A, links.lww.com/NXI/A706). Five weeks of cuprizone intoxication resulted also in T2-weighted CC signal increases by 53% (Figure 1B). After cuprizone withdrawal at week 5, the T2-weighted signal intensity (T2-WSI) was reduced in the CC at weeks 5–7 (Figure 1D), consistent with spontaneous partial remyelination and reduction of neuroinflammation in these areas.²⁷ Addition of siponimod to food pellets increased

Figure 1 Siponimod Therapy Promotes Remyelination After Toxic Demyelination by Cuprizone



(A) Longitudinal body weight changes in all study groups. (B) T2-WSI after 5 weeks. (C) Longitudinal MRI monitoring for magnetization transfer ratio changes in the CC. (D) Longitudinal T2-WSI monitoring for T2-WSI changes in the CC of mice in all study groups. Changes are expressed as mean \pm SEM ($n = 7$ animals per group), and gray dots show individual data points. Magnet symbol indicates the timing for the MRI readouts. *** $p < 0.001$ compared by ANOVA with the Dunnett post hoc test for area under the curve bar graph and * $p < 0.05$ and *** $p < 0.001$ by ANOVA with random effects compared with the cuprizone/sham group for time courses. ANOVA = analysis of variance.

this reduction of T2-WSI (Figure 1D) with a significant difference to siponimod-free pellet treated mice in the CC. This effect was again particularly evident when analyzing the AUC (eFigure 1B). T2-WSI in the CC of control mice remained unaltered. Both MTR and T2-WSI data of the CC indicate the beneficial effects of siponimod treatment in the cuprizone model. Terminal qIHC for LFB density and oligodendrocyte numbers (GST- π) revealed a degree of myelination in the CC reduced by about half in cuprizone-challenged mice receiving drug-free food pellets vs controls. A trend toward a lower degree of CC demyelination was observed in siponimod-treated mice, with changes in LFB density and oligodendrocyte numbers reduced by about 25–45% vs siponimod-free mice (eFigure 1).

Siponimod-Driven Activation of S1P1/5 Receptor Promotes Remyelination

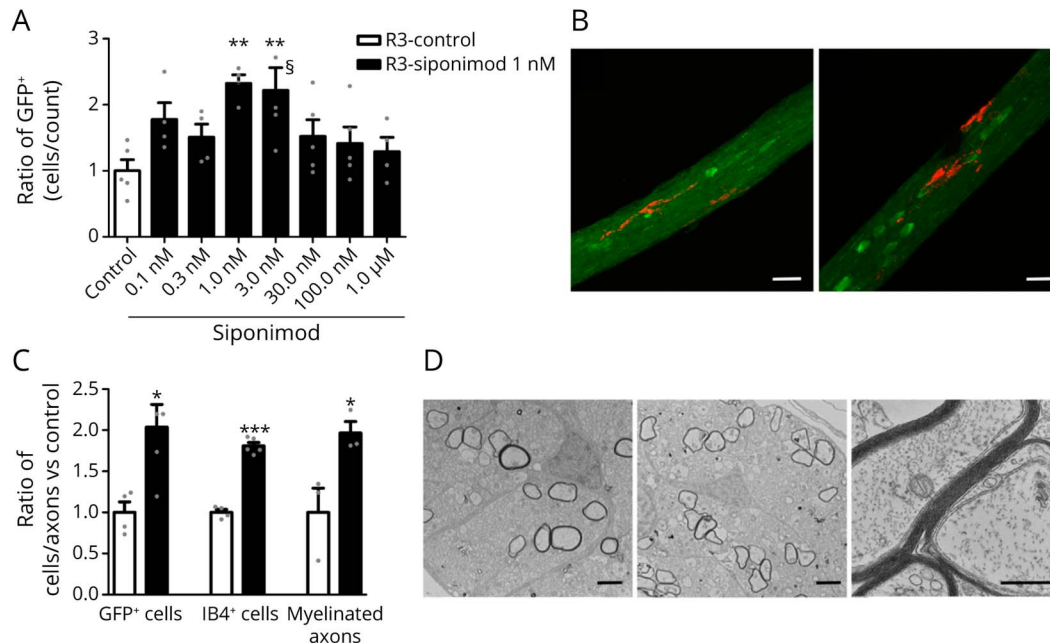
Conditional oligodendrocyte ablation and demyelination followed by spontaneous remyelination was investigated in the Tg(mbp:GFP-NTR) *Xenopus laevis* model, and the dynamics are reported in eAppendix 1 and eFigure 2, links.lww.com/NXI/A706. Demyelination and remyelination were analyzed by counting the number of GFP+ cells per optic nerve in vivo before (D0), at the end of MTZ treatment (D10), and then on day 3 (R3) of the repair period. To assess remyelination potency

on stopping MTZ exposure, siponimod was added in the swimming water at nominal doses ranging from 0.1 nM to 1 μ M. Under these conditions, siponimod accumulated over time in tadpole tissues in a dose-proportional manner reaching mean levels of 30–60 pmol/g (equivalent to 30–60 nM) at nominal doses \leq 3 nM, whereas mean tissues exposures equivalent to 0.6, 1.7, and 36 μ M were achieved at the nominal dose of 0.03, 0.1, and 1 μ M, respectively. Of interest, at all nominal doses tested, similar siponimod levels were measured in brain vs body samples, with a mean brain/body ratio of 0.9 ± 0.3 .

Siponimod treatments, at nominal doses from 0.1 to 3 nM, improved remyelination in a dose-dependent manner, with a maximal and significant 2.3 ± 0.2 fold increase vs control observed at the nominal dose of 1 nM (i.e., achieving about 60 nM accumulated in tissues over 3 days). At nominal doses $>$ 3 nM (i.e., $>$ 60 nM in tissues), the promyelination effect of siponimod reduced markedly in a dose-dependent manner, with nearly no trend observed at nominal doses \geq 30 nM (i.e., 600 nM accumulated in tissues), revealing an unclassical bell-shaped overall dose-response curve for siponimod in this remyelination model (Figure 2A).

In addition to S1P5, siponimod acts also on S1P1, a receptor expressed by microglia. To explore the effect of siponimod

Figure 2 Spontaneous Remyelination of Transgenic *Xenopus laevis* With Siponimod Treatment; Effects on Microglia, Oligodendrocytes, and Remyelination



Stage 52–53 transgenic Tg(mbp:GFP-NTR) *Xenopus laevis* tadpoles were exposed for 10 days in metronidazole (10 mM) before being returned in normal water or water containing increasing concentrations of siponimod. (A) Remyelination was assayed by counting the number of GFP + oligodendrocytes per optic nerve in vivo on day 3 (R3) of the repair period (n = 5–8 tadpoles per group). (B and C) After demyelination, animals were returned for 3 days to either normal water (Ctrl) or water containing siponimod (1 nM). Confocal images of oligodendrocytes (GFP+ green) and microglia (IB4+ red) in the optic nerve following spontaneous recovery (B, left) or siponimod treatment (B, right). Quantification of the effects of siponimod treatment on the number of myelin-forming (C, GFP+) oligodendrocytes and (C, IB4+) microglia (ctrl n = 4; siponimod n = 6). Electron micrograph of transversally cut optic nerve 3 days after either (D, left) spontaneous recovery or (D, middle) siponimod treatment. (D, right) Higher magnification of ongoing remyelination under siponimod treatment showing axons ensheathed with increasing number of myelin wraps. (C, myelinated axons) Quantification of the number of myelinated axons per optic nerve following siponimod treatment vs control of spontaneous remyelination (n = 5). Data are expressed as mean \pm SEM, and gray dots show individual data points. ** $p < 0.01$ calculated using 1-way ANOVA, followed by the Dunn post hoc test for (A) compared with control (Ctrl) condition. For C with * $p < 0.05$ and *** $p < 0.001$ (Student 2-tailed unpaired t test). Scale bars: B = 20 μ m; D = 2 μ m. §One data point out of axis limits. ANOVA = analysis of variance.

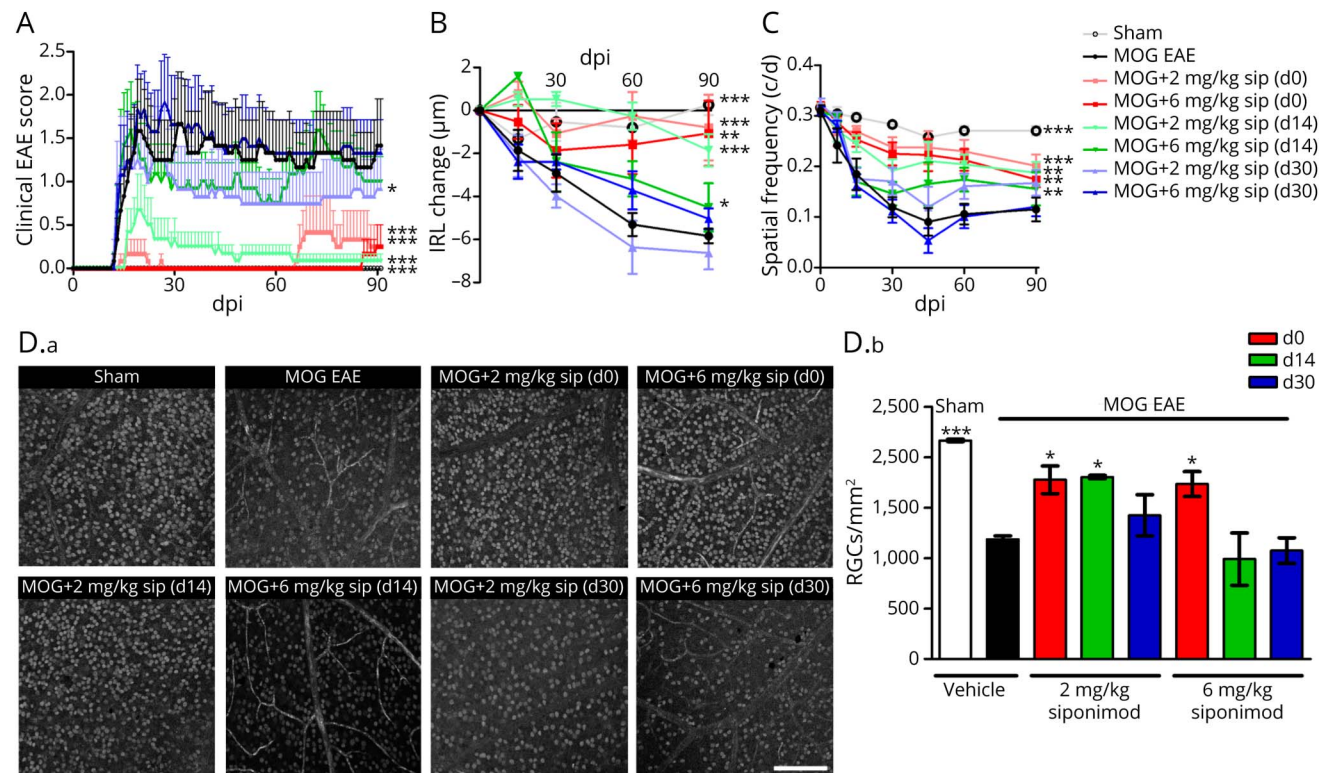
treatment on microglial cells, transgenic Tg(mbp:GFP-NTR) *Xenopus* were demyelinated by 10-day exposure to MTZ (10 mM) and then returned to either normal water or water containing siponimod (1 nM) for 3 days. Optic nerves were dissected and doubly labeled with IB4 isolectin and anti-GFP (Figures 2, B and C). In addition to the expected increase (2.04 fold vs ctrl $p = 0.017$) in the number of GFP+ cells, we also observed a 1.81 fold increase ($p < 0.0001$) in the number of IB4-labeled microglial cells (Figure 2C). After 3 days of recovery, microglial cells presented with an elongated morphology, extending their processes along the optic nerve, and we did not notice a change in the morphology of microglia on siponimod treatment (Figure 2B).

To verify that the siponimod-induced increased number of oligodendrocytes (GFP+ cells) translated into increased myelination, optic nerves were dissected and processed for electron microscopy. The number of myelinated axons quantified on semithin sections was nearly doubled (1.97 ± 0.14 fold vs ctrl; $p = 0.042$) (Figure 2C), and there was no noticeable morphologic changes compared with control conditions (Figure 2D).

Siponimod Reduces the Disability Score and Retinal Degeneration in an EAEON Model

Before investigating the effects of siponimod on EAEON, we performed a pharmacokinetic study, which demonstrated that treatment by loaded food pellets was superior to supply by drinking water and showed a robust effect on circulating blood cell counts in flow cytometry (eAppendix 1, eFigure 3, and eFigure 4, links.lww.com/NXI/A706). After observing these promising data in the cuprizone and the *Xenopus laevis* demyelination models, we longitudinally investigated retinal neurodegeneration in MOG₃₃₋₅₅ peptide-induced EAEON in C57BL/6J mice over 90 days to test the potential of siponimod to protect from acute inflammatory relapses, as well as chronic degeneration, similar to the progression of SPMS. In this model, prophylactic siponimod treatment acted beneficially on clinical EAE scores with more pronounced effects compared with therapeutic treatment. Siponimod prophylactic diet treatments at 2 and 6 mg/kg BW attenuated the clinical EAE scores by approximately 80% and 95%, respectively. The therapeutic effect was significant with the lower dose (2 mg/kg) at both time points and when started at d14 almost similar to the prophylactic treatment (Figure 3A).

Figure 3 Siponimod Attenuates Myelin Oligodendrocyte Glycoprotein Fragment 35-55-Induced EAE in C57BL/6J Mice in a Dose- and Time-Dependent Manner



(A) Clinical EAE score, (B) degeneration of the inner retinal layers, and (C) visual function by spatial frequency in cycles per degree (c/d) of female C57BL/6J EAE mice over 90 days of EAE. (D.a) Brn3a stained RGCs after 90 days of EAE of Sham-, MOG EAE-, and siponimod-treated mice, scale bar = 200 µm. (D.b) The bar graph shows the RGC density 90 days after immunization. Siponimod was administered either on the day of immunization (d0), 14 days (d14) or 30 days (d30) post immunization (dpi). All graphs represent the pooled mean \pm SEM, and gray dots show individual data points (out of 2 independent experiments each with $n = 6$ animals per group) with $*p < 0.05$, $**p < 0.01$, and $***p < 0.001$, area under the curve compared by generalized estimating equation or ANOVA with the Dunnett post hoc test for time courses compared with untreated MOG EAE. $*p < 0.05$ and $***p < 0.001$ by ANOVA with the Dunnett post hoc test compared with MOG EAE untreated mice for the bar graph. ANOVA = analysis of variance; EAE = experimental autoimmune encephalomyelitis; MOG = myelin oligodendrocyte glycoprotein; RGC = retinal ganglion cell.

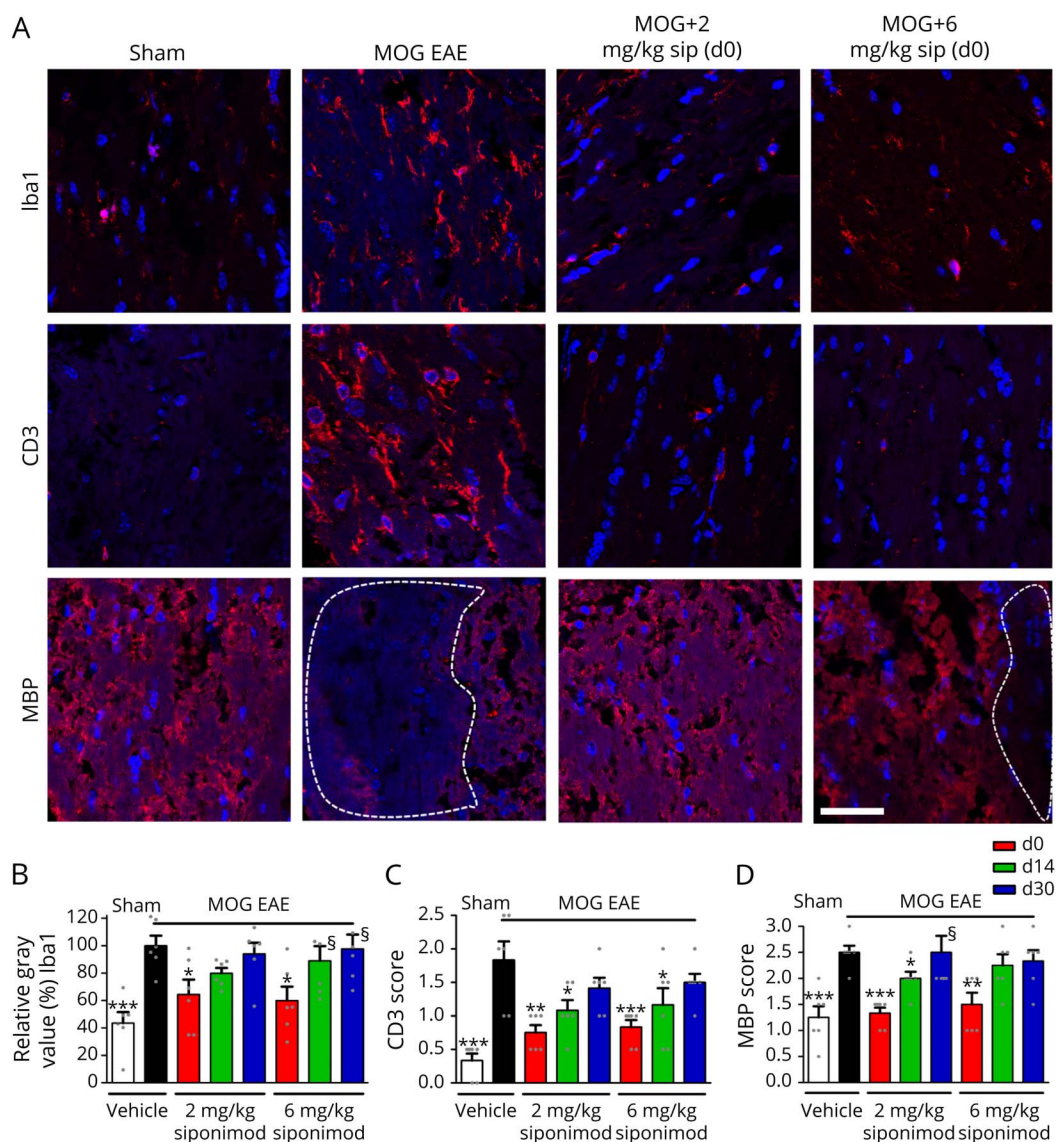
Analyzing the structural changes by OCT, untreated sham control mice showed a nearly constant IRL thickness, whereas MOG peptide-immunized animals presented a prominent loss of IRL thickness until day 90. Prophylactic siponimod therapy at 2 and 6 mg/kg BW reduced the OCT-measured degeneration of the IRL by approximately 50%. Beneficial effects were observed with therapeutic diet treatments starting at day 14, with 2 mg/kg BW being superior over 6 mg/kg BW ($p < 0.01$), but not at day 30 (Figure 3B). Analyzing the visual acuity, a strong decrease of spatial frequency over 90 days of vehicle-treated MOG EAE mice was revealed. This was significantly prevented by almost all therapeutic interventions, despite the late treatment (d30) with the higher dose (6 mg/

kg) of siponimod (Figure 3C). These effects, measured longitudinally in vivo, were well reflected by the investigation of RGC survival 90 days postimmunization (dpi). Prominent RGC loss of untreated EAE animals was diminished by siponimod prophylactic diet, as well as therapeutic treatment with 2 mg/kg, but not 6 mg/kg starting 14 dpi (Figure 3D).

Siponimod Prevents Inflammation and Demyelination of the Optic Nerve

To assess the effects of siponimod on immune cell infiltration into the CNS during EAE, we performed histologic analyses of Iba1⁺ microglia/macrophages and CD3⁺ T cells in longitudinal optic nerve sections (Figure 4A). A significant

Figure 4 Prophylactic Siponimod Therapy Reduces Immune Cell Infiltration and Prevents Demyelination



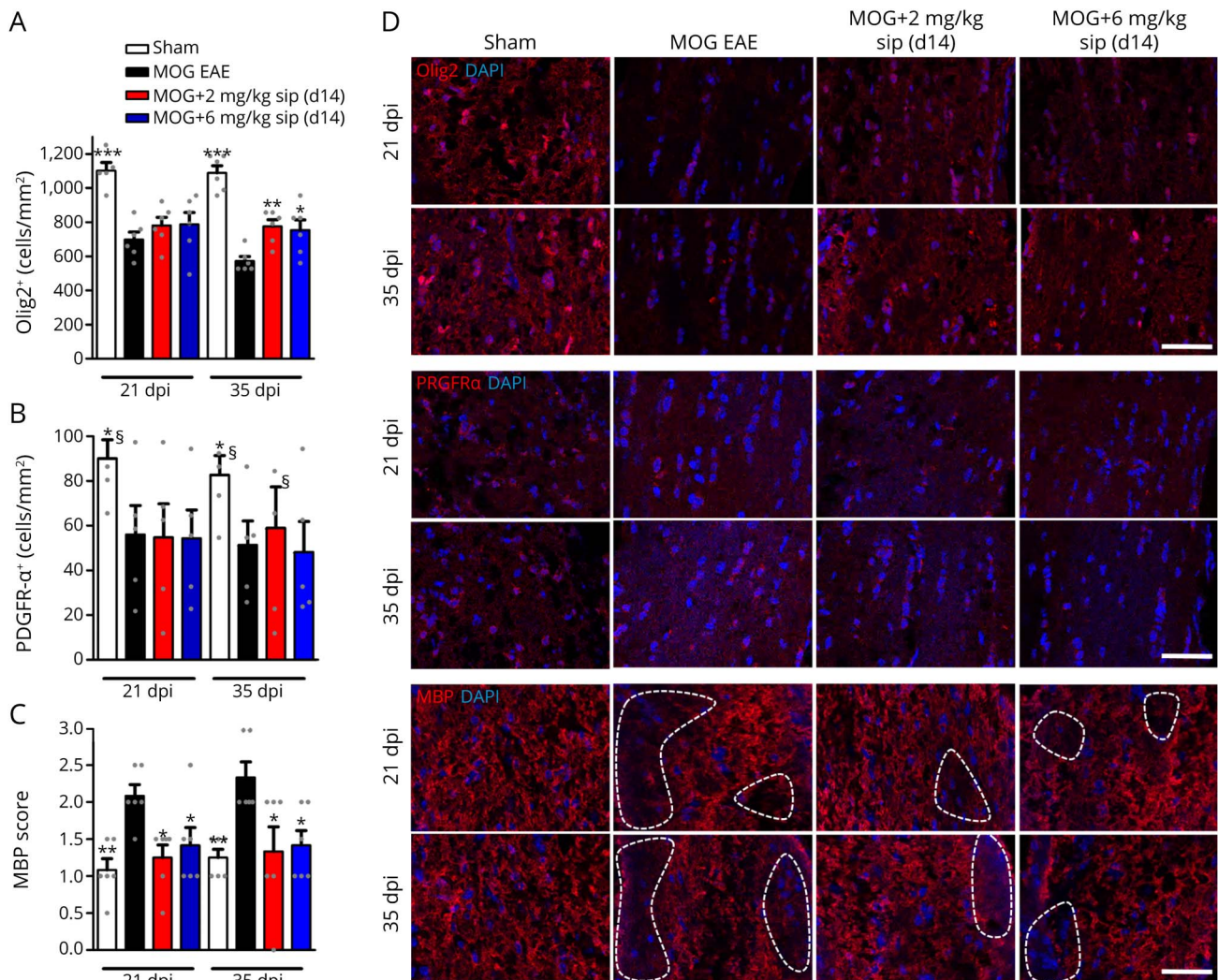
(A) Longitudinal sections of optic nerves of C57Bl/6j mice were stained for Iba1, CD3, and MBP 90 days after myelin oligodendrocyte glycoprotein fragment 35-55 immunization; dotted lines indicate areas of demyelination, scale bar = 50 μ m. Quantitative analyses of microglial activation (Iba1, B) by fluorescence intensity measurement, T-cell infiltration (CD3 score, C), and myelin status (MBP score, D). One optic nerve per mouse was included. All graphs represent the pooled mean \pm SEM, and gray dots show individual data points (n = 6 animals per group out of 2 independent experiments), with * $p < 0.05$, ** $p < 0.01$, and *** $p < 0.001$ by ANOVA with the Dunnett post hoc test compared with myelin oligodendrocyte glycoprotein untreated mice. §Few data points out of axis limits. ANOVA = analysis of variance.

reduction of microglial/macrophage activity as well as T-cell infiltration was observed in the optic nerves of mice after prophylactic (d0) siponimod treatment compared with untreated EAE mice. Interventions at later time points did not diminish the infiltrating Iba1⁺ cells (Figure 4B). Nevertheless, a therapeutic siponimod treatment at the peak of disease (d14) led to a less severe infiltration of CD3⁺ lymphocytes compared with MOG EAE vehicle-treated mice. When the mice were fed with siponimod-loaded pellets from 30 days after MOG immunization, the number of immune cells could not be reduced at 2 or 6 mg/kg BW (Figure 4C). To test the capacity of siponimod to prevent from demyelination, we analyzed the myelin status of the optic nerve by performing immunohistologic stainings against the myelin basic protein (MBP) protein. The axonal tissue of MOG-immunized mice

presented large areas of demyelination, whereas the optic nerves from untreated sham mice showed a homogeneous myelin structure. The MBP-stained lesions in the optic nerve were significantly reduced after a prophylactic siponimod therapy, showing almost the same uniform pattern as sham control animals. Even late siponimod therapy (d14) showed a beneficial effect at 2 mg/kg BW, whereas a treatment starting at day 30 had no significant effect on the myelin loss during EAEON in C57Bl/6J mice until 90 days after immunization (Figures 4, A and D).

Extended analysis of oligodendrocyte populations revealed that siponimod (d14) improved survival of Olig2⁺ cells in the optic nerve after 35 dpi compared with untreated MOG EAE mice (Figures 5, A and D). As a marker for OPCs, PDGFR α -

Figure 5 Siponimod Also Reduces Early Demyelination but Does Not Alter Oligodendrocyte Precursor Cell Survival



Quantitative analysis of longitudinal sections of optic nerves of C57Bl/6J mice for (A) Olig2, (B) PDGFR α , and (C) MBP at 21 and 35 days after myelin oligodendrocyte glycoprotein fragment 35-55 immunization. Representative images of the stainings (D); dotted lines indicate areas of demyelination, scale bar = 50 μ m. One optic nerve per mouse was included for histologic examination. All graphs represent the pooled mean \pm SEM, and gray dots show individual data points (n = 6 animals per group out of 2 independent experiments), with * p < 0.05, ** p < 0.01, and *** p < 0.001 by ANOVA with the Dunnett post hoc test compared with untreated myelin oligodendrocyte glycoprotein experimental autoimmune encephalomyelitis. §Few data points out of axis limits. ANOVA = analysis of variance.

stained cells showed no difference in cell number when we compared untreated and siponimod-treated EAE mice at 2 and 6 mg/kg BW, whereas sham control mice had higher OPC numbers at 21 and 35 dpi (Figures 5, B and D). Similar as after 90 dpi, early demyelination was reduced after siponimod therapy for both doses (Figures 5, C and D). Increased astrogliosis in the optic nerve, analyzed by GFAP staining, was observed in MOG EAE mice after 21 and 35 dpi, whereas no effect of siponimod was observed (eFigure 5, links.lww.com/NXI/A706).

In the retina of the mice, we assessed microglia (Iba1) and astrocyte/Mueller cell (GFAP) appearance also 90 days after MOG immunization. We found an increased number of Iba1+ cells in untreated EAEON animals compared with sham mice, but only observed a significant decrease for microglial numbers at the 2 mg/kg BW siponimod dose (d0) (eFigure 6, links.lww.com/NXI/A706).

Siponimod Shifts Microglia to a Promyelinating Phenotype

As siponimod still had beneficial effects on the MBP level even in the therapeutic approach (d14), we expanded the expression and histologic analysis in the optic nerve, testing genes involved in oligodendrocyte as well as microglial regulation. After siponimod treatment (2 mg/kg BW), we found significant upregulation in the optic nerve mRNA expression level 35 dpi of genes marking OPCs NG2 and PDGFR α , as well as for the markers for resting microglia CD206 and TMEM 119 (eFigure 7, A and B, links.lww.com/NXI/A706), which could, however, not be corroborated on the protein level by histologic examinations. Chitinase-3-like-3 (Chi3l3/Ym1) and arginase-1 (Arg-1) mRNA levels were significantly upregulated 21 and 35 dpi, especially after treatment with 2 mg/kg BW siponimod compared with MOG EAE-untreated mice (eFigure 7, C and D). Both are markers for regeneration-supporting microglia. Similar results were observed in BV2 cells, a microglial cell line, where Ym1 and Arg-1 mRNA levels were upregulated after siponimod treatment (eFigure 8, A and B). In addition, mRNA levels of TNF- α , a cytokine expressed by activated, proinflammatory microglia, were significantly reduced after siponimod therapy compared with untreated EAE mice (eFigure 7E). The transcriptional regulation was mirrored by the histologic examination of the optic nerve, where Ym1 (Figures 6, A and D) and Arg-1 (Figure 6, B and D) were found upregulated 21 and 35 dpi after siponimod treatment with a trend toward a more potent effect of the lower siponimod dose (2 mg/kg BW). TNF- α was significantly upregulated in the optic nerve of EAE animals with a peak at 35 dpi, whereas mice under siponimod therapy showed a significantly lower expression of TNF- α (Figures 6, C and D).

RNA Sequencing Analysis of the EAEON Optic Nerve Reveals Downregulation of Genes Associated With Inflammation After Siponimod Treatment

In a completely unbiased approach, we used bulk RNA sequencing of the optic nerve of EAEON animals with and

without siponimod treatment at 21 dpi, starting the therapy 14 days after immunization (d14). *p* Values were adjusted for multiple testing to control the false discovery rate (FDR) ($p\text{FDR} < 0.05$), and fold change (FC) was set to 1.5. In a heat map, showing the differentially expressed genes (DEGs), sham and MOG EAE animals show a fully altered expression profile, whereas the DEGs of MOG- and siponimod-treated mice (2 mg/kg) are more similar (Figure 7A).

Comparing sham with MOG EAE animals, an upregulation of 2,109 genes and a downregulation of 623 genes were observed, displayed in a volcano plot (Figure 7B). After the siponimod treatment, we found a downregulation of 129 genes and an upregulation of 1 gene after treatment with 2 mg/kg BW siponimod (Figure 7C) and a downregulation of 106 genes with 6 mg/kg BW siponimod compared with untreated MOG EAE control. The 5 most differentially expressed genes associated with inflammation are summarized in eTable 2, links.lww.com/NXI/A706.

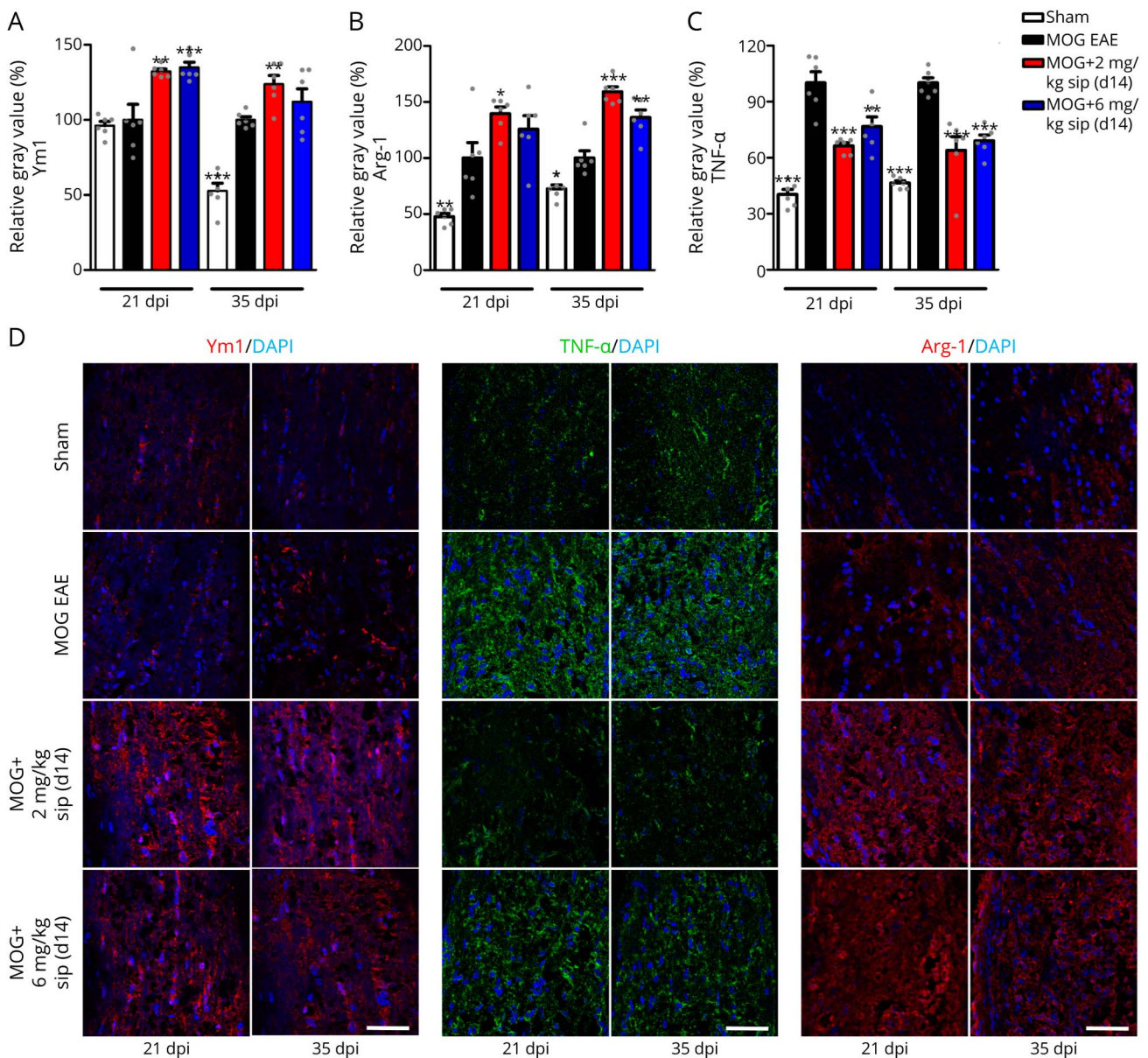
Discussion

Although the early disease progression in MS can be effectively prevented or mitigated by immunomodulatory therapy, there is still an unmet need for remyelinating strategies and substances to attenuate or inhibit the degeneration occurring in the later stages.²⁸ Siponimod has recently demonstrated efficacy in SPMS.¹

As a first step, the remyelinating potential of siponimod after toxic demyelination by cuprizone was investigated by MRI of the corpus callosum. MTR and T2-WSI measurements at 1 week after cuprizone withdrawal demonstrated significant beneficial effects of siponimod treatment on CC integrity. Other studies with the more unspecific S1P1 receptor modulator fingolimod reported a downregulation of S1PR1 brain levels, and fingolimod-treated mice presented more oligodendrocytes in the secondary motor cortex after 3 weeks of remyelination. However, no differences in remyelination or axonal damage were observed compared with placebo.²⁹ In a novel MS model, a combination of EAE and cuprizone intoxication, siponimod mitigated the extent of demyelination.³⁰

To further assess the remyelinating potential of siponimod, we used an inducible experimental model developed in *Xenopus laevis*. After demyelination of the *Xenopus* tadpoles over 10 days, spontaneous remyelination occurred. However, remyelination was significantly accelerated by siponimod in a bell-shaped dose-response curve. We had previously shown that in both the mouse and *Xenopus* brain, S1PR5 is only expressed by oligodendrocytes and that the remyelinating potency of siponimod is lost on deletion of S1PR5.^{15,31} It is therefore likely that the mechanism of action of siponimod-induced remyelination is by activating the myelination program of oligodendrocyte through activation of S1PR5. In addition, as S1P1 is also expressed on microglia,³² a cell

Figure 6 Siponimod Therapy Shifts Microglia to a Regenerative Phenotype

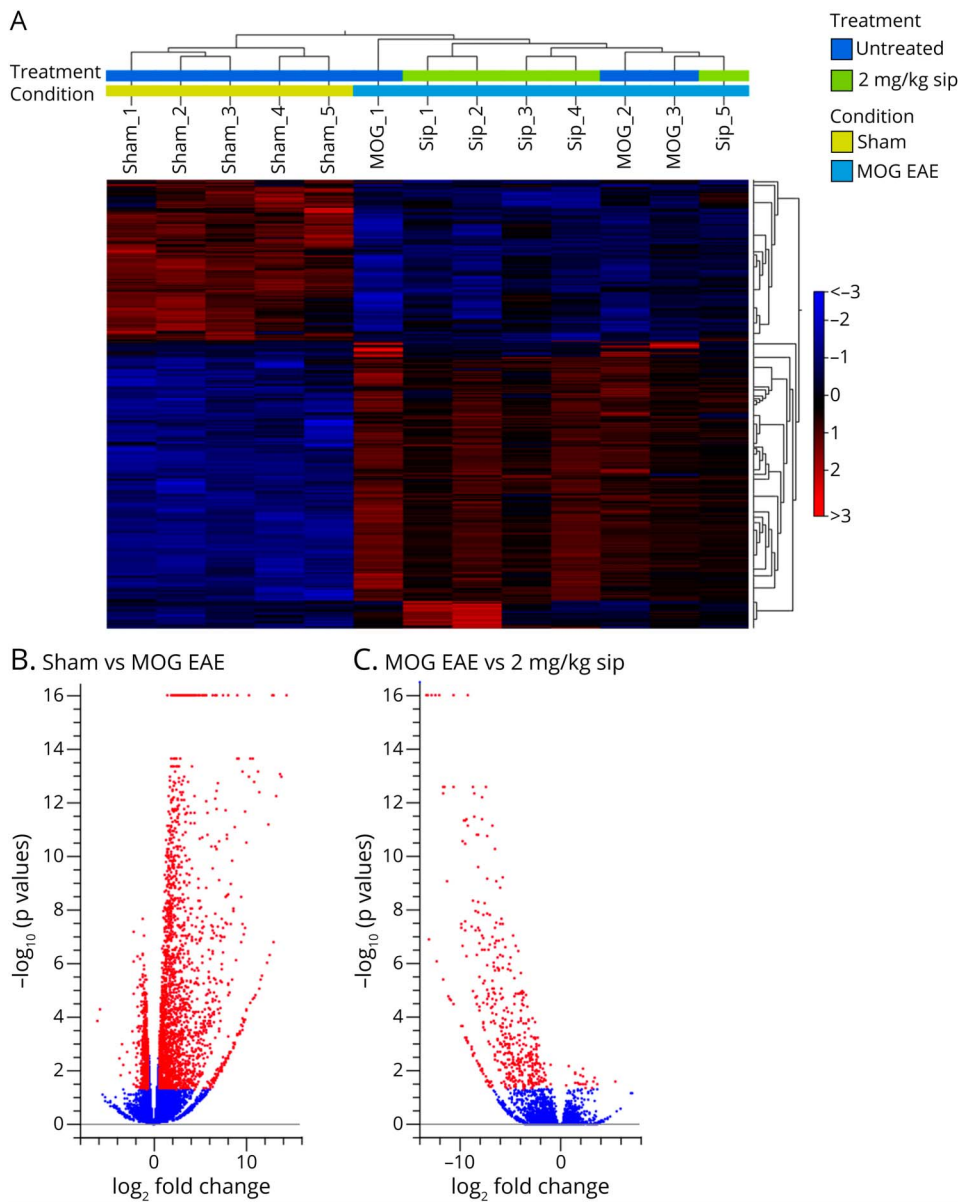


Quantitative analysis of longitudinal sections of optic nerves of C57Bl/6j mice for Ym1 (A), TNF- α (B), and Arg-1 (C) at 21 and 35 days after myelin oligodendrocyte glycoprotein fragment 35-55 immunization. Representative images of the stainings (D), scale bar = 50 μ m. One optic nerve per mouse was included for histologic examination. All graphs represent the pooled mean \pm SEM, and gray dots show individual data points ($n = 6$ animals per group out of 2 independent experiments), with $*p < 0.05$, $**p < 0.01$, and $***p < 0.001$ compared by ANOVA with the Dunnett post hoc test compared with untreated myelin oligodendrocyte glycoprotein experimental autoimmune encephalomyelitis. ANOVA = analysis of variance.

population required during spontaneous remyelination,³³ we also investigated their regulation after siponimod treatment. An increased number of IB4⁺ microglia were observed presenting an elongated morphology 3 days after recovery. In line with this hypothesis, recent observations suggest that in contrast to the S1P1 receptor, the S1P5 receptor is not subject to agonist-induced downmodulation and that siponimod should be considered as a true S1P5 agonist.³⁴ In this case, a phenomenon such as S1P5 desensitization at supramaximal stimulation could be suspected to explain the bell-shaped curve for the promyelination effect of siponimod.

After these promising results, we then moved to mouse EAE models to investigate the effects in a more disease specific model with translational potential. Siponimod crosses the blood-brain barrier and targets different S1P receptor subtypes, associated with T-cell migration into the CNS, astrogliosis, repair mechanisms via modulation of S1PRS on oligodendrocytes, and cell survival.^{35,36} Hence, the EAEON model in mice appears as a perfectly suited mechanistic tool to assess the impact of siponimod on all these central effects. In this model, a significant attenuation of the clinical EAE score with 2 and 6 mg/kg BW was observed, when the therapy was

Figure 7 Gene Expression Profile of Optic Nerves of MOG EAE- and Siponimod-Treated Mice at 21 Dpi



(A) Hierarchical clustering of differentially expressed genes after sham, MOG EAE, and MOG with 2 mg/kg BW siponimod treatment. Red indicates increased expression, and blue indicates decreased expression. Differences in expression were set to $FC \geq 1.5$, with $p(\text{FDR}) < 0.05$. Volcano plot showing differentially expressed genes 21 dpi for (B) sham compared with MOG EAE animals and (C) MOG EAE compared with MOG with 2 mg/kg siponimod. For each plot, the x-axis represents \log_2 FC, and the y-axis represents $-\log_{10}(p \text{ values})$. DEGs are shown as red dots. EAE = experimental autoimmune encephalomyelitis; MOG = myelin oligodendrocyte glycoprotein.

initiated at the day of immunization, in line with previous approaches, using various EAE models in mice and rats.^{2,37-39} To explore effects of siponimod beyond its immunomodulatory capacity, we not only used different dosing paradigms but also started the siponimod diet at prophylactic (d0) and early or late therapeutic (d14/d30) time points. Other studies addressing similar issues varied only one of these parameters and started treatment no later than 8 days after EAE immunization.³⁸ A significant beneficial effect on the EAE score was observed when treatment was started at days 14 and 30 after MOG immunization, but surprisingly only with the lower concentration (2 mg/kg BW), indicating a bell-shaped dose-effect curve. We already identified the same dose dependency in a rat MOG₂₈₋₁₅₂-induced EAE in C57Bl/6J mice, where the same dosing (10 mg/kg food or 2 mg/kg BW) led to the most effective reduction of

the EAE score of 72.5%,^{18,20} with robust dose-proportional CNS penetration and distribution for siponimod.¹⁸ As preclinical study designs with readouts directly transferable to clinical trials are of increasing interest and other preclinical studies on siponimod's central effects lack of these techniques, we included visual system measurements to evaluate the results. The IRL, consisting of the RNFL, GCL and IPL contains the axons of the optic nerve, ganglion cells and their dendritic arbor, and is the ideal structure to study neuroprotection and retinal degeneration in MS,^{6,9,40} as well as in preclinical EAEON studies.^{10-12,17,41} As functional readout, the OMR is a suitable measure for the visual acuity in rodents.^{17,23,42} Although IRL degeneration was attenuated by a prophylactic and a therapeutic 2 mg/kg BW treatment starting 14 dpi, the visual function was even preserved by a therapeutic regimen starting at 30 dpi. This observation was

mirrored by the number of RGCs, as the loss of these cells was significantly diminished by prophylactic, but also therapeutic siponimod therapy, mainly by the lower dose of 2 mg/kg BW, also observed in similar studies.⁴³⁻⁴⁵

The reduced number of circulating T cells led to a decreased infiltration of CD3⁺ cells into the optic nerve, if the intervention was started not later than d14. A therapy at d30 still reduced the circulating T cells by a significant level, but the infiltration into the optic nerve, mainly occurring around days 11–14 at the peak of the EAEON,⁴¹ could not be prevented. Antidemyelinating effects, also observed by other researchers in mouse organotypic slice cultures,³⁶ were detected after prophylactic siponimod treatment at both doses and interestingly also after therapeutic treatment with 2 mg/kg BW. As S1P receptors, with the exception of S1P5, are also expressed on microglial cells,³² we expected a reduced number of Iba1-positive cells in the optic nerve after siponimod treatment. However, this effect was only observed after prophylactic therapy, which can be explained by the fact that microgliosis is already present as early as 7 dpi in EAEON.⁴¹ We therefore extended the histologic investigations on genes associated with oligodendrocyte and microglial regulation. We found no transcriptional regulation of genes regulating oligodendrocyte maturation and myelination at the early time points of 21 and 35 dpi. On the other hand, histologic stainings of the optic nerve revealed an improved Olig2+ cell survival at 35 dpi and a less pronounced demyelination at 21 and 35 dpi, measured by the MBP score, similar as at the end point of 90 dpi. Together with the result that no regulation of PDGFR α positive cells by siponimod was found, this indicates an effect of the drug on mature oligodendrocytes rather than on OPCs. Furthermore, we observed significant upregulation of the microglial regenerative markers Ym1 and Arg-1 and a downregulation of the proinflammatory cytokine TNF- α on a transcriptional and translational level at 21 and 35 dpi after siponimod therapy in the optic nerve. In mice, Ym1 is highly expressed in inflammatory brain lesions during EAE and has been demonstrated to induce oligodendrogenesis.⁴⁶ Thus, it seems reasonable to assume that the observed beneficial effects of siponimod on the myelin status, observed at 90 dpi may, at least in part, be resulting from its effects on microglial cells, shifting them to a promyelinating phenotype. This is in line with the assumption that the beneficial effects of siponimod go beyond lymphocyte trafficking and rely on its interactions with other cells of the CNS, like astrocytes and neurons, as the drug crosses the blood-brain barrier and S1P receptors are expressed on almost all CNS cell types.⁴⁷

In addition to the targeted investigations of oligodendroglial and microglial genes and proteins, we also applied an unbiased approach, analyzing the transcriptome of the optic nerve by bulk RNAseq. It was striking that 129 and 106 genes were downregulated, whereas only 1 and no gene were upregulated after 2 and 6 mg/kg BW siponimod treatment in EAEON, respectively. Significantly downregulated genes potentially altering the disease progression were associated with inflammation. We decided to perform a bulk RNAseq of the whole optic nerve to receive a cell-unspecific, unbiased overview on DEGs after siponimod treatment of EAEON mice. However, a more targeted approach

sequencing single cells, such as oligodendrocytes, microglia, or astrocytes, might have led to more homogeneous and conclusive results. As we focused our EAEON study on in vivo readouts of the visual system, the histology and transcriptomic analyses were also focused on the optic nerve. We acknowledge that also investigating the spinal cord may have yielded additional information, but this would have been beyond the focus of this study.

Taken together, these observations suggest a beneficial effect of siponimod in the CNS by shifting microglia to a regenerative phenotype and protective effect on oligodendrocytes, in line with the promyelination effects observed in the *Xenopus laevis* model.

In summary, siponimod demonstrated increased remyelination in the CC in the cuprizone demyelination model, promyelination potential in the *Xenopus* model, and strong prophylactic and therapeutic effects in the mouse EAEON, as revealed by visual (functional and structural) readouts. Having used 3 experimental models in 2 different animal species strengthens our results in favor of a remyelinating potential for siponimod in MS.

Acknowledgment

France: The authors thank the ARSEP foundation, FRM (Fondation pour la Recherche Médicale), Bouvet-Labruyere Family, INSERM-DHOS, APHP (Assistance Publique des Hôpitaux de Paris), the program “Investissements d’Avenir” ANR-10-IAIHU-06, NeurATRIS, ANR grant BRECOMY to B.Z., and NRJ foundation for their precious support related to basic and clinical research on remyelination in Paris. Novartis: the authors thank Claire Moebs, Catherine Afatsawo, Desrayaud Sandrine, Hager Claude, Neuhaus Anna, Lang Meike, Perrot Ludovic, Rudin Stefan, Wipfli Peter, and Zurbruegg Stefan for their key scientific and operational support. Germany: computational support of the Zentrum für Informations-und Medientechnologie, especially the HPC team (High Performance Computing) at the Heinrich Heine University, is acknowledged. The authors also thank Thorsten Wachtmeister for technical support and Zippora Kohne for technical assistance.

Study Funding

This work was supported by grants to PA from Novartis Pharma GmbH, the charitable Iselore-Lückow Stiftung, and the charitable Dr.-Robert-Pfleger Stiftung. The study was partially funded by a research grant from Novartis to BZ and the European Union’s Horizon 2020 Research and Innovation Programme ENDpoiNTs project Grant Agreement number: 825759 and grant BRECOMY funded jointly by DFG and ANR to BZ.

Disclosure

M. Dietrich received speaker honoraria from Merck. M. Gliem has received honoraria for speaking/consultation from Bayer HealthCare and Boehringer Ingelheim and a research grant from B. Braun, outside the submitted work. B. Stankoff has received compensation for boards and/or lectures from Biogen, Sanofi Genzyme, Novartis, and Teva and research grants from Merck, Roche, and Sanofi Genzyme. C. Lubetzki has participated in advisory boards for Vertex, Roche, Biogen, Novartis, Genzyme,

and Merck and speaking honoraria from Ipsen and Biogen. P. Göttle performed consultancy work for GeNeuro and received support from the Research Commission of the medical faculty of the Heinrich Heine University. H.P. Hartung has received fees for serving on steering and data monitoring committees from Bayer HealthCare, Biogen, Celgene BMS, CSL Behring, GeNeuro, MedImmune, Merck, Novartis, Octapharma, Roche, Sanofi Genzyme, TG Therapeutics, and Viela Bio, fees for serving on advisory boards from Biogen, Sanofi Genzyme, Merck, Novartis, Octapharma, and Roche, and lecture fees from Biogen, Celgene BMS, Merck, Novartis, Roche, and Sanofi Genzyme. P. Kury performed consultancy work for GeNeuro and received support from Sanofi Genzyme, French societies ARSEP and AFM, Deutsche Forschungsgemeinschaft (DFG; grants KU1934/2_1, KU1934/5-1), Stifterverband/Novartisstiftung, and from James and Elisabeth Cloppenburg, Peek and Cloppenburg Düsseldorf Stiftung. S.G. Meuth received honoraria for lecturing and travel expenses for attending meetings from Almirall, Amicus Therapeutics Germany, Bayer HealthCare, Biogen, Celgene, Diamed, Genzyme, MedDay Pharmaceuticals, Merck Serono, Novartis, Novo Nordisk, ONO Pharma, Roche, Sanofi-Aventis, Chugai Pharma, QuintilesIMS, and Teva; his research is funded by the German Ministry for Education and Research (BMBF), Deutsche Forschungsgemeinschaft (DFG), Else Kröner Fresenius Foundation, German Academic Exchange Service, Hertie Foundation, Interdisciplinary Center for Clinical Studies (IZKF) Muenster, German Foundation Neurology, and by Almirall, Amicus Therapeutics Germany, Biogen, Diamed, Fresenius Medical Care, Genzyme, Merck Serono, Novartis, ONO Pharma, Roche, and Teva. B. Zalc received research support from Novartis and Merck and travel grant from Merck. P. Albrecht received compensation for serving on scientific advisory boards for Ipsen, Novartis, and Biogen; he received speaker honoraria and travel support from Novartis, Teva, Biogen, Merz Pharmaceuticals, Ipsen, Allergan, Bayer HealthCare, Esai, UCB, and GlaxoSmithKline; he received research support from Novartis, Biogen, Teva, Merz Pharmaceuticals, Ipsen, and Roche. P. Ramseier, C. Beerli, S. Tisserand, N. Beckmann, D. Shimshek, and M. Bigaud are employees of the Novartis Institutes for BioMedical Research; the other authors report no disclosures. Go to Neurology.org/NN for full disclosures.

Publication History

Received by *Neurology: Neuroimmunology & Neuroinflammation* September 20, 2021. Accepted in final form January 27, 2022. Submitted and externally peer reviewed. The handling editor was Scott S. Zamvil, MD, PhD, FAAN.

Appendix Authors

Name	Location	Contribution
Michael Dietrich, PhD	Department of Neurology, Heinrich Heine University Düsseldorf, Medical Faculty, Düsseldorf, Germany	Drafting/revision of the manuscript for content, including medical writing for content; major role in the acquisition of data; study concept or design; and analysis or interpretation of data

Appendix (continued)

Name	Location	Contribution
Christina Hecker, MSc	Department of Neurology, Heinrich Heine University Düsseldorf, Medical Faculty, Düsseldorf, Germany	Major role in the acquisition of data and analysis or interpretation of data
Elodie Martin, PhD	Sorbonne Université, Inserm, CNRS, Institut du Cerveau, Pitié-Salpêtrière Hospital	Major role in the acquisition of data
Dominique Langui, PhD	Sorbonne Université, Inserm, CNRS, Institut du Cerveau, Pitié-Salpêtrière Hospital	Major role in the acquisition of data and analysis or interpretation of data
Michael Gliem, MD	Department of Neurology, Heinrich Heine University Düsseldorf, Medical Faculty, Düsseldorf, Germany	Analysis or interpretation of data
Bruno Stankoff, MD, PhD, PU-PH	Sorbonne Université, Inserm, CNRS, Institut du Cerveau, Pitié-Salpêtrière Hospital; AP-HP, Saint-Antoine Hospital	Analysis or interpretation of data
Catherine Lubetzki, MD, PhD, PU-PH	Sorbonne Université, Inserm, CNRS, Institut du Cerveau, Pitié-Salpêtrière Hospital; AP-HP, Pitié-Salpêtrière Hospital, Paris, France	Analysis or interpretation of data
Joel Gruchot, MSc	Department of Neurology, Heinrich Heine University Düsseldorf, Medical Faculty, Düsseldorf, Germany	Major role in the acquisition of data and analysis or interpretation of data
Peter Göttle, PhD	Department of Neurology, Heinrich Heine University Düsseldorf, Medical Faculty, Düsseldorf, Germany	Major role in the acquisition of data and analysis or interpretation of data
Andrea Issberner	Department of Neurology, Heinrich Heine University Düsseldorf, Medical Faculty, Düsseldorf, Germany	Major role in the acquisition of data
Milad Nasiri, MD	Department of Neurology, Heinrich Heine University Düsseldorf, Medical Faculty, Düsseldorf, Germany	Major role in the acquisition of data
Pamela Ramseier	Novartis Institutes for BioMedical Research, Basel, Switzerland	Major role in the acquisition of data
Christian Beerli	Novartis Institutes for BioMedical Research, Basel, Switzerland	Major role in the acquisition of data
Sarah Tisserand, MSc	Novartis Institutes for BioMedical Research, Basel, Switzerland	Major role in the acquisition of data and analysis or interpretation of data
Nicolau Beckmann, PhD	Novartis Institutes for BioMedical Research, Basel, Switzerland	Drafting/revision of the manuscript for content, including medical writing for content; major role in the acquisition of data; and analysis or interpretation of data
Derya Shimshek, PhD	Novartis Institutes for BioMedical Research, Basel, Switzerland	Major role in the acquisition of data and analysis or interpretation of data

Continued

Appendix (continued)

Name	Location	Contribution
Patrick Petzsch, PhD	Biological and Medical Research Center (BMFZ), Heinrich Heine University Düsseldorf, Medical Faculty	Major role in the acquisition of data and analysis or interpretation of data
David Akbar, MSc	Sorbonne Université, Inserm, CNRS, Institut du Cerveau, Pitié-Salpêtrière Hospital	Major role in the acquisition of data
Bodo Levkau, Prof.	Institute for Molecular Medicine III, University Hospital Düsseldorf and Heinrich Heine University Düsseldorf	Drafting/revision of the manuscript for content, including medical writing for content, and analysis or interpretation of data
Holger Stark, Prof.	Institute of Pharmaceutical and Medicinal Chemistry, Heinrich Heine University Düsseldorf, Duesseldorf, Germany	Drafting/revision of the manuscript for content, including medical writing for content, and analysis or interpretation of data
Karl Köhrer, Prof.	Biological and Medical Research Center (BMFZ), Heinrich Heine University Düsseldorf, Medical Faculty	Analysis or interpretation of data
Hans-Peter Hartung, Prof.	Department of Neurology, Heinrich Heine University Düsseldorf, Medical Faculty, Düsseldorf, Germany; Brain and Mind Center, University of Sydney, NSW, Australia; Medical University of Vienna, Vienna, Austria	Drafting/revision of the manuscript for content, including medical writing for content, and analysis or interpretation of data
Patrick Küry, Prof.	Department of Neurology, Heinrich Heine University Düsseldorf, Medical Faculty, Düsseldorf, Germany	Drafting/revision of the manuscript for content, including medical writing for content; major role in the acquisition of data; and analysis or interpretation of data
Sven Günther Meuth, Prof.	Department of Neurology, Heinrich Heine University Düsseldorf, Medical Faculty, Düsseldorf, Germany	Drafting/revision of the manuscript for content, including medical writing for content, and analysis or interpretation of data
Marc Bigaud, PhD	Novartis Institutes for BioMedical Research, Basel, Switzerland	Drafting/revision of the manuscript for content, including medical writing for content; major role in the acquisition of data; study concept or design; and analysis or interpretation of data
Bernard Zalc, Prof.	Sorbonne Université, Inserm, CNRS, Institut du Cerveau, Pitié-Salpêtrière Hospital	Drafting/revision of the manuscript for content, including medical writing for content; major role in the acquisition of data; study concept or design; and analysis or interpretation of data
Philipp Albrecht, Prof.	Heinrich Heine University Düsseldorf, Medical Faculty, Düsseldorf, Germany	Drafting/revision of the manuscript for content, including medical writing for content; major role in the acquisition of data; study concept or design; and analysis or interpretation of data

References

- Kappos L, Bar-Or A, Cree BAC, et al. Siponimod versus placebo in secondary progressive multiple sclerosis (EXPAND): a double-blind, randomised, phase 3 study. *Lancet*. 2018;391(10127):1263-1273.
- Gentile A, Musella A, Bullitta S, et al. Siponimod (BAF312) prevents synaptic neurodegeneration in experimental multiple sclerosis. *J Neuroinflammation*. 2016;13(1):207.
- Lubetzki C, Zalc B, Williams A, Stadelmann C, Stankoff B. Remyelination in multiple sclerosis: from basic science to clinical translation. *Lancet Neurol*. 2020;19(8):678-688.
- Franklin RJM, Ffrench-Constant C. Regenerating CNS myelin - from mechanisms to experimental medicines. *Nat Rev Neurosci*. 2017;18(12):753-769.
- Zhan J, Mann T, Joost S, Behrangi N, Frank M, Kipp M. The cuprizone model: dos and do not. *Cells*. 2020;9(4).
- Albrecht P, Ringelstein M, Müller AK, et al. Degeneration of retinal layers in multiple sclerosis subtypes quantified by optical coherence tomography. *Mult Scler*. 2012;18(10):1422-1429.
- Gabilondo I, Martínez-Lapiscina EH, Martínez-Heras E, et al. Trans-synaptic axonal degeneration in the visual pathway in multiple sclerosis. *Ann Neurol*. 2014;75(1):98-107.
- Saidha S, Al-Louzi O, Ratchford JN, et al. Optical coherence tomography reflects brain atrophy in multiple sclerosis: a four-year study. *Ann Neurol*. 2015;78(5):801-813.
- Albrecht P, Fröhlich R, Hartung HP, Kieseier BC, Methner A. Optical coherence tomography measures axonal loss in multiple sclerosis independently of optic neuritis. *J Neurol*. 2007;254(11):1595-1596.
- Dietrich M, Koska V, Hecker C, et al. Protective effects of 4-aminopyridine in experimental optic neuritis and multiple sclerosis. *Brain*. 2020;143(4):1127-1142.
- Cruz-Herranz A, Dietrich M, Hilla AM, et al. Monitoring retinal changes with optical coherence tomography predicts neuronal loss in experimental autoimmune encephalomyelitis. *J Neuroinflammation*. 2019;16(1):203.
- Knier B, Rothhammer V, Heink S, et al. Neutralizing IL-17 protects the optic nerve from autoimmune pathology and prevents retinal nerve fiber layer atrophy during experimental autoimmune encephalomyelitis. *J Autoimmun*. 2014;56:34-44.
- Diem R, Molnar F, Beisse F, et al. Treatment of optic neuritis with erythropoietin (TONE): a randomised, double-blind, placebo-controlled trial-study protocol. *BMJ Open*. 2016;6(3):e010956.
- Kaya F, Mannioui A, Chesneau A, et al. Live imaging of targeted cell ablation in Xenopus: a new model to study demyelination and repair. *J Neurosci*. 2012;32(37):12885-12895.
- Mannioui A, Vauzanges Q, Fini JB, et al. The Xenopus tadpole: an in vivo model to screen drugs favoring remyelination. *Mult Scler*. 2018;24(11):1421-1432.
- Martin E, Aigrot MS, Grenningloh R, et al. Bruton's tyrosine kinase inhibition promotes myelin repair. *Brain Plast*. 2020;5(2):123-133.
- Dietrich M, Helling N, Hilla A, et al. Early alpha-lipoic acid therapy protects from degeneration of the inner retinal layers and vision loss in an experimental autoimmune encephalomyelitis-optic neuritis model. *J Neuroinflammation*. 2018;15(1):71.
- Bigaud M, Rudolph B, Briard E, et al. Siponimod (BAF312) penetrates, distributes, and acts in the central nervous system: preclinical insights. *Mult Scler J Exp Transl Clin*. 2021;7(4):20552173211049168.
- Bachmanov AA, Reed DR, Beauchamp GK, Tordoff MG. Food intake, water intake, and drinking spout side preference of 28 mouse strains. *Behav Genet*. 2002;32(6):435-443.
- Bigaud M, Perdoux J, Ramseier P, Tisserand S, Urban B, Beerli C. Pharmacokinetic/Pharmacodynamic characterization of siponimod (BAF312) in blood versus brain in experimental autoimmune encephalomyelitis mice (P2.2-066). *Neurology*. 2019;92:15.
- Bigaud M, Tisserand S, Ramseier P, et al. Differentiated pharmacokinetic/pharmacodynamic (PK/PD) profiles for Siponimod (BAF312) versus Fingolimod. 2019. Poster (P622) presented at: 35th Congress of the European Committee for Treatment and Research in Multiple Sclerosis, September 11-13, 2019, Stockholm, Sweden.
- Dietrich M, Cruz-Herranz A, Yiu H, et al. Whole-body positional manipulators for ocular imaging of anaesthetised mice and rats: a do-it-yourself guide. *BMJ Open Ophthalmol*. 2017;1(1):e000008.
- Dietrich M, Hecker C, Hilla A, et al. Using optical coherence tomography and optokinetic response as structural and functional visual system readouts in mice and rats. *J Vis Exp*. 2019;143(143).
- Cruz-Herranz A, Balk LJ, Oberwahrenbrock T, et al. The APOSTEL recommendations for reporting quantitative optical coherence tomography studies. *Neurology*. 2016;86(24):2303-2309.
- Prusky GT, Alam NM, Beekman S, Douglas RM. Rapid quantification of adult and developing mouse spatial vision using a virtual optomotor system. *Invest Ophthalmol Vis Sci*. 2004;45(12):4611-4616.
- Lewerenz J, Albrecht P, Tien ML, et al. Induction of Nrf2 and xCT are involved in the action of the neuroprotective antibiotic ceftriaxone in vitro. *J Neurochem*. 2009;111(2):332-343.
- Beckmann N, Giorgetti E, Neuhaus A, et al. Brain region-specific enhancement of remyelination and prevention of demyelination by the CSF1R kinase inhibitor BLZ945. *Acta Neuropathol Commun*. 2018;6(1):9.
- Vargas DL, Tyor WR. Update on disease-modifying therapies for multiple sclerosis. *J Investig Med*. 2017;65(5):883-891.
- Nystad AE, Lereim RR, Wergeland S, et al. Fingolimod downregulates brain sphingosine-1-phosphate receptor 1 levels but does not promote remyelination or neuroprotection in the cuprizone model. *J Neuroimmunol*. 2020;339:577091.

30. Behrangi N, Atanasova D, Kipp M. Siponimod ameliorates inflammation and axonal injury in a novel multiple sclerosis model. 2019. Poster (P512) presented at: 35th Congress of the European Committee for Treatment and Research in Multiple Sclerosis, September 11-13, 2019, Stockholm, Sweden.
31. Jaillard C, Harrison S, Stankoff B, et al. Edg8/S1P5: an oligodendroglial receptor with dual function on process retraction and cell survival. *J Neurosci.* 2005;25(6):1459-1469.
32. Tham CS, Lin FF, Rao TS, Yu N, Webb M. Microglial activation state and lysophospholipid acid receptor expression. *Int J Dev Neurosci.* 2003;21(8):431-443.
33. Miron VE, Boyd A, Zhao JW, et al. M2 microglia and macrophages drive oligodendrocyte differentiation during CNS remyelination. *Nat Neurosci.* 2013;16(9):1211-1218.
34. Bigaud M, Tisserand S, Fuchs-Loesle P, Guerini D. The S1P5 receptor is not downmodulated in response to selective agonists. 2018. Poster (EP1617) presented at: 34th Congress of the European Committee for Treatment and Research in Multiple Sclerosis, October 10-12, 2019, Berlin, Germany.
35. Bigaud M, Guerini D, Billich A, Bassilana F, Brinkmann V. Second generation S1P pathway modulators: research strategies and clinical developments. *Biochim Biophys Acta.* 2014;1841(5):745-758.
36. O'Sullivan C, Schubart A, Mir AK, Dev KK. The dual S1PR1/S1PR5 drug BAF312 (Siponimod) attenuates demyelination in organotypic slice cultures. *J Neuroinflammation.* 2016;13:31.
37. Gergely P, Nuesslein-Hildesheim B, Guerini D, et al. The selective sphingosine 1-phosphate receptor modulator BAF312 redirects lymphocyte distribution and has species-specific effects on heart rate. *Br J Pharmacol.* 2012;167(5):1035-1047.
38. Ward LA, Lee DS, Sharma A, et al. Siponimod therapy implicates Th17 cells in a preclinical model of subpial cortical injury. *JCI Insight* 2020;5(1):e132522.
39. Hundehage P, Cerina M, Eichler S, et al. The next-generation sphingosine-1 receptor modulator BAF312 (siponimod) improves cortical network functionality in focal autoimmune encephalomyelitis. *Neural Regen Res.* 2019;14(11):1950-1960.
40. Dietrich M, Aktas O, Hartung HP, Albrecht P. Assessing the anterior visual pathway in optic neuritis: recent experimental and clinical aspects. *Curr Opin Neurol.* 2019;32(3):346-357.
41. Manogaran P, Samardzija M, Schad AN, et al. Retinal pathology in experimental optic neuritis is characterized by retrograde degeneration and gliosis. *Acta Neuropathol Commun.* 2019;7(1):116.
42. Hecker C, Dietrich M, Issberner A, Hartung HP, Albrecht P. Comparison of different optomotor response readouts for visual testing in experimental autoimmune encephalomyelitis-optic neuritis. *J Neuroinflammation.* 2020;17(1):216.
43. McDougald DS, Dine KE, Zezulin AU, Bennett J, Shindler KS. SIRT1 and NRF2 gene transfer mediate distinct neuroprotective effects upon retinal ganglion cell survival and function in experimental optic neuritis. *Invest Ophthalmol Vis Sci.* 2018;59(3):1212-1220.
44. Smith AW, Rohrer B, Wheless L, et al. Calpain inhibition reduces structural and functional impairment of retinal ganglion cells in experimental optic neuritis. *J Neurochem.* 2016;139(2):270-284.
45. Larabee CM, Desai S, Agasing A, et al. Loss of Nrf2 exacerbates the visual deficits and optic neuritis elicited by experimental autoimmune encephalomyelitis. *Mol Vis* 2016; 22:1503-1513.
46. Starossom SC, Campo Garcia J, Woelfle T, et al. Chi3l3 induces oligodendrogenesis in an experimental model of autoimmune neuroinflammation. *Nat Commun.* 2019; 10(1):217.
47. Behrangi N, Fischbach F, Kipp M. Mechanism of siponimod: anti-inflammatory and neuroprotective mode of action. *Cells.* 2019;8(1):24.